J|A|C|S
COMMUNICATIONS

Published on Web 09/16/2004

Plasmon Mode Imaging of Single Gold Nanorods

Kohei Imura,[†,‡] Tetsuhiko Nagahara,[†] and Hiromi Okamoto*[,†,‡]

Institute for Molecular Science, Okazaki 444-8585, Japan, and
The Graduate University for Advanced Studies, Okazaki 444-8585, Japan

Received April 15, 2004; E-mail: aho@ims.ac.jp

Photoluminescence (PL) from noble metal films was first reported in 1969.[1] Similar PL was also observed in surface-enhanced Raman scattering (SERS) experiments,[2] and it renewed interest in PL from the noble metals. Boyd et al.[3] investigated the excitation-energy dependence and the effect of surface roughness on the PL of noble metallic films and found that local field enhancement due to surface plasmon (SP) resonance is a prerequisite for PL. In this sense, PL from metals has strong analogies to SERS. Strong field confinement also occurs in the vicinity of noble metal particles,[4] and local field enhancement up to 10^{15} was reported.[5] However, the spatial distribution of the electric field near the particle and how plasmon modes play roles in the particle are still not fully understood. Very recently, two-photon-induced photoluminescence (TPI−PL) of contacted gold nanoparticles (dimer) was reported.[6] However, TPI−PL of individual nanoparticles has not been reported. Observation of TPI−PL from single nanoparticles may bring essential information for revealing the spatial distribution of the electric field near the particle, since the two-photon process is more sensitive to the local field strength than the single-photon process. The electric field near the particle should be correlated to the plasmon modes. Therefore, it is also expected that TPI−PL is useful for investigation of spatial characteristics of the plasmon modes. In this communication, we present TPI−PL spectroscopy and imaging of single gold nanorods by using an apertured scanning near-field optical microscope (SNOM). The results reveal characteristic features of plasmon modes in PL images and also enable us to obtain knowledge of electric field distributions around the nanorod.

Gold nanorods were synthesized chemically in solutions by seed-mediated method according to Murphy and co-workers.[7] Morphology of the sample was verified by topography measurements by the SNOM and/or by a scanning electron microscope. Samples were spin-coated on a cover-slip after removing most of surfactants from the sample solution (10^{-3} to 10^{-4} of the original solution). The present configuration of measurement is described in Supporting Information. Briefly, an apertured SNOM was used. A Ti:sapphire laser ($\lambda = 780$ nm, <100 fs) was used to excite TPI−PL. Emitted PL was collected by an objective and detected either by an avalanche photodiode with optical filters (340−620 nm) or by a polychromator-CCD to acquire the PL spectrum. Laser power dependence measurement of the PL intensity confirmed that PL was due to a two-photon-induced process.

Figure 1 shows a TPI−PL spectrum measured for a single gold nanorod excited at wavelength 780 nm. Two peaks are clearly seen in Figure 1. As is well-known, PL in a solid is a three-step process. The process begins with electron−hole pair excitation. In the next step, relaxation of the initially excited electron and hole to new energy states occurs via a manifold of scattering processes in metal. Finally, emission is radiated when the electron and hole recombine.

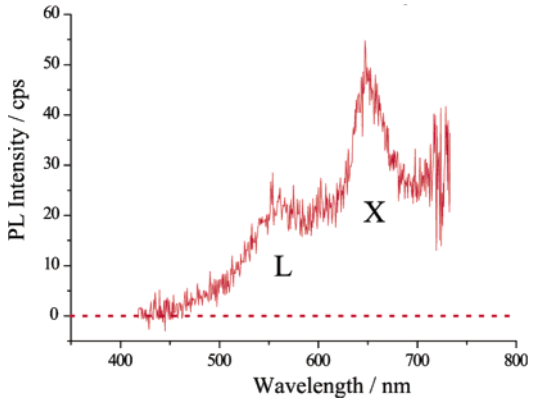

Figure 1. Two-photon-induced photoluminescence (PL) spectrum of a single gold nanorod. The dotted line shows a baseline at substrate.

Electron−hole recombination effectively occurs between the excited electrons near the Fermi surface and holes in the d band. The peak energy of the emitted photons is therefore closely connected to the energy separation between the Fermi surface and the holes in the d band. In the gold crystal, it is expected that optical transitions preferentially occur near the X and L symmetry points of the first Brillouin zone, since the density of states near these symmetry points are high.[8] According to the calculated band structure of gold,[9] emission peaks are expected to be observed near 650 and 520 nm in wavelengths for the regions of the X and L symmetry points, respectively.[3] The two peaks observed in Figure 1 are thus assigned to the electron−hole recombination near the X and L symmetry points, respectively. The relative intensities of these spectral components (I_X and I_L, respectively) vary for each particle. The observed ratio I_X/I_L ranges roughly from 0.5 to 2. The spectral intensity depends on the electromagnetic local density of states (LDOS) of the nanorod and the magnitude of transition matrix elements. As the LDOS must be strongly correlated to SP modes (eigenfunctions) in the nanorod, variation of the relative intensities of the two spectral components may be related to the difference in the plasmon modes excited.

Figures 2a,b show topographic images of gold nanorods. These images are broadened due to convolution of a near-field probe tip. Dotted squares indicate approximate shapes of the rods estimated from the topographic images, considering the broadening effect by the tip. The estimated rod dimensions (diameter × length) are ca. 40 × 230 nm for Figure 2a and ca. 35 nm × 440 nm for Figure 2b. The uncertainty of the estimated dimensions is about ±10%. In the shorter rod in Figure 2c, the TPI−PL is enhanced in both ends of the rod. This spatial distribution may be arising from electric field enhancement near the ends of the rod. In the longer rod in Figure 2d, on the other hand, the PL intensity shows characteristic spatial oscillation along the long axis. Similar oscillating patterns were also found for the other nanorods. Typical spacing between the bright spots ranged from 100 to 140 nm and depended on the

[†] Institute for Molecular Science.
[‡] The Graduate University for Advanced Studies.

10.1021/ja047836c CCC: $27.50

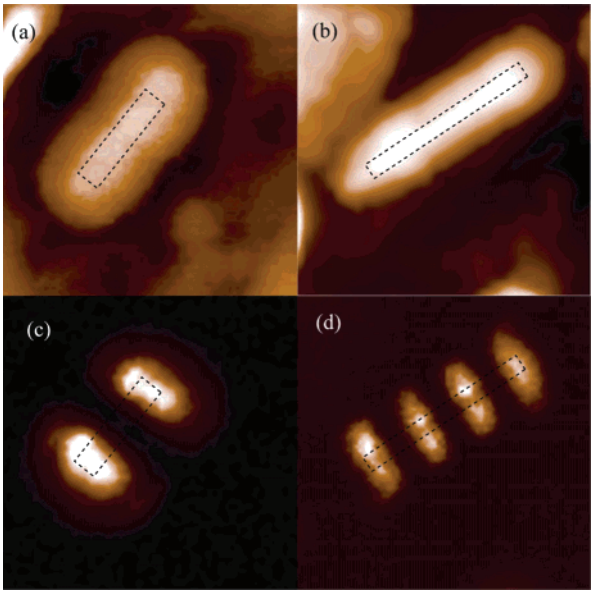

Figure 2. (a,b) Topographic images of gold nanorods. (c,d) Two-photon-induced PL images for a and b, respectively. Image sizes are 600 × 600 nm (a,c) and 700 × 700 nm (b,d).

rod diameter. Aperture diameters used for Figures 2c and 2d are ca. 100 and 70 nm, respectively. Here we have shown in Figures 2c and 2d two representative images, but we have measured many other (more than 50) gold nanorods, including those with different lengths. It has been confirmed that similar propensity is found for other gold nanorods.

The excitation probability of PL in the particle should be a product of a two-photon absorption probability and a field enhancement strength (due probably to the microscopic structure of the rod edge). The two-photon absorption probability at a given position in the particle is considered to be reflected on electromagnetic LDOS. The oscillatory structure found in Figure 2d may therefore originate in spatial characteristics of LDOS of the nanorod. In fact, it has been theoretically predicted, using electric Green dyadic method (GDM),[10,11] that LDOS in noble metal nanowire systems exhibit distinct oscillations along the wire axes, which are related to certain SP modes.[12,13] We have simulated the spatial distribution of LDOS for the nanorod corresponding to Figure 2d using GDM.[14] Separation of calculated LDOS maxima has been found to be ca. 100 nm for the excitation wavelength of 780 nm, in good agreement with the observed separation between bright spots in Figure 2d. This agreement suggests that the excitation probability of PL in the particle shown in Figure 2b is explained primarily by the factor of two-photon absorption probability and that the oscillatory structure reflects the eigenfunction of the SP mode. It is to be noted that the contrast of the intensity profile along the long axis is very sharp in the PL image, in comparison with the calculated LDOS profile.[12] This may be related to the nonlinear character of the two-photon process, and it would enhance spatial resolution. It is also to be noted that PL intensity at the end parts is comparable to that of the middle parts. This implies that the field enhancement at the end parts does not give significant contribution to excitation probability.

Such an observation of a SP mode is only attained when the incident light locally excites the nanorod and at the same time the excitation is coherent over the whole rod. If the nanorod is entirely excited by a far-field incident light, the LDOS profile along the nanorod is smeared out because of low spatial resolution and/or the forbidden character of local-mode excitation.

On the other hand, for the shorter rod in Figure 2a, the observed separation between the bright spots in Figure 2c is ca. 190 nm, while that between calculated LDOS maxima is ca. 100−150 nm for a nanorod of 220 nm in length. This serious discrepancy suggests that the two-photon excitation probability is mainly controlled by the field enhancement effects in both edges for the rod in Figure 2a. The situation is quite different from the longer rod in Figure 2b. Even in the longer rods with sizes similar to that in Figure 2b, we sometimes have observed only the enhancements in the edge. In this case, the separation between the bright spots was about 500 nm. The origin of the difference is possibly related to microscopic structures of the rod and/or the resonance condition of the plasmon mode at the excitation wavelength, but this is not clear yet. Further investigations are necessary to clarify this point.

In summary, we have investigated the TPI−PL of gold nanorods by an apertured SNOM. Observed PL spectra of the gold nanorods can be explained by the radiative recombination of the electron−hole pair near the X and L symmetry points. A PL image for a short rod reveals that the strong field enhancement occurs at the end parts of the rod. A PL image for a longer rod shows characteristic features reflecting an eigenfunction of a specific plasmon mode and gives good correspondence with calculated electromagnetic LDOS.

Acknowledgment. This study was partly supported by Grants-in-Aid for Scientific Research (16350015, 16750017) from Japan Society for the Promotion of Science.

Supporting Information Available: Details of experimental setup and image contrast discussion (PDF). This material is available free of charge via the Internet at http://pubs.acs.org.

References

(1) Mooradian, A. *Phys. Rev. Lett.* **1969**, *22*, 185−187.
(2) (a) Birke, R. L.; Lombardi, J. R.; Gersten, J. I. *Phys. Rev. Lett.* **1979**, *43*, 71−75. (b) Burstei, E.; Chen, Y. J.; Chen, C. Y.; Lundquist, S.; Tossati, E. *Solid State Commun*. **1979**, *29*, 567−570. (c) Otto, A. *Surf. Sci*. **1978**, *85*, L392−396. (d) Tsang, J. C.; Kirtley, J. R.; Theis, T. N. *Solid State Commun*. **1980**, *35*, 667−670.
(3) Boyd, G. T.; Yu, Z. H.; Shen, Y. R. *Phys. Rev. B*. **1986**, *33*, 7923−7936.
(4) (a) Michaels, A. M.; Nirmal, M.; Brus, L. E. *J. Am. Chem. Soc*. **1999**, *121*, 9932−9939. (b) Kennedy, B. J.; Spaeth, S.; Dickey, M.; Carron, K. T. *J. Phys. Chem. B* **1999**, *103*, 3640−3646. (c) Nikoobakht, B.; El-Sayed, M. A. *J. Phys. Chem. A* **2003**, *107*, 3372−3378.
(5) Nie, S.; Emory, S. R. *Science* **1997**, *275*, 1102−1106.
(6) Bouhelier, A.; Beversluis, M. R.; Novotny, L. *Appl. Phys. Lett*. **2003**, *83*, 5041−5043.
(7) (a) Jana, N. R.; Gearheart, L.; Murphy, C. J. *J. Phys. Chem. B* **2001**, *105*, 4065−4067. (b) Busbee, B. D.; Obare, S. O.; Murphy, C. J. *Adv. Mater*. **2003**, *15*, 414−416.
(8) Guerrisi, M.; Rosei, R.; Winsemius, P. *Phys. Rev. B*. **1975**, *12*, 557−563.
(9) Christensen, N. E.; Seraphin, B. O. *Phys. Rev. B*. **1972**, *4*, 3321−3344.
(10) Girard, C.; Dereux, A. *Rep. Prog. Phys*. **1996**, *59*, 657−699.
(11) Greffet, J.-J.; Carminati, R. *Prog. Sur. Sci*. **1997**, *56*, 133−237.
(12) Weeber, J.-C.; Dereux, A.; Girard, C.; Krenn, J. R.; Goudonnet, J.-P. *Phys. Rev. B*. **1999**, *60*, 9061−9068.
(13) (a) Podolskiy, V. A.; Sarychev, A. K.; Shalaev, V. M. *J. Nonlinear Opt. Phys. Mater*. **2002**, *11*, 65−74. (b) Podolskiy, V. A.; Sarychev, A. K.; Shalaev, V. M. *Opt. Express* **2003**, *11*, 735−745.
(14) Imura, K.; Nagahara, T.; Okamoto, H. *J. Phys. Chem. B*. ASAP Article (jp047950h).

JA047836C